

Dynamic Effective Electron-Electron Interaction in the Vicinity of a Polarizable Molecule*

W. A. Little

Stanford University, Stanford, California 94305

and

H. Gutfreund

Department of Theoretical Physics, Hebrew University, Jerusalem, Israel

(Received 24 February 1971)

A method is described for calculating the effective electron-electron interaction in the vicinity of a polarizable molecule. The technique is applied to a numerical calculation of this interaction for dye molecules which are possible candidates for providing the attractive interaction for the proposed excitonic superconductor. The frequency and spatial dependence of this interaction is calculated, and a useful upper limit is obtained for the strength of the interaction near a single dye. Good agreement is found between the calculated and observed oscillator strengths, which indicates that these methods can provide a useful guide for precise calculations of the coupling strength for any proposed model system.

I. INTRODUCTION

In an earlier series of papers, referred to hereafter as I, II, and III,¹⁻³ we considered the effects of correlations among the π electrons in large conjugated hydrocarbons and the effects that these would have upon the effective electron-electron interaction between electrons in these molecules. The principle motivation for this was a need for more accurate methods for calculating the energy levels and transition densities of highly polarizable molecules, which are of interest as candidates for providing the excitonic interaction in a proposed high-temperature superconducting material.^{4,5} Earlier work by one of us⁴ had used an extremely crude and naive form of molecular orbital theory in considering that problem, and it was upon the outcome of these calculations that it was concluded that high-temperature superconductivity could be expected in certain macromolecular systems. The approximate nature of those calculations was criticized by Paulus,⁶ as was the final conclusion. The purpose of the present paper is to reexamine this problem or, more precisely, to examine the detailed nature of the dynamic effective interaction between charges in the vicinity of a highly polarizable molecules, such as a dye using the more sophisticated techniques of I, II, and III. We consider how closely one can explain theoretically the experimentally observable behavior of these dyes, and discuss the degree of precision one can place upon the effective interaction calculated by these means. We examine the spatial variation of this interaction in order to determine how such molecules might be used effectively to provide an excitonic attraction between electrons in a neighboring conductive medium. Because of the many imaginable conformations in which an array of such dyes might be found, we

have not attempted to discuss the complete problem of both the conductive medium and the dye array. We leave that to a later paper.

One of us has argued^{4,5} that a net attractive interaction between two electrons should result if these electrons are confined to move in the vicinity of a highly polarizable medium. The attraction arises in a similar manner to that induced by the phonon-electron interaction in a superconducting metal. In such a metal one electron polarizes the neighboring ionic medium, while the second is attracted to the polarization cloud. Because of the inertia of the ions, the attractive component of the net interaction is delayed in time compared to the nearly instantaneous Coulomb repulsive component, and for this reason the attractive component can dominate. In the proposed excitonic mechanism the lattice ionic polarizability is replaced by an electronic polarizability. Similar arguments to the above apply to this case except that the time scales are shorter and the energies involved appreciably larger.

II. DYNAMIC EFFECTIVE INTERACTION

We consider then the problem of calculating the dynamic effective interaction between two charges in the neighborhood of a polarizable molecule. This interaction has two parts: first, a component due to the instantaneous Coulomb repulsion between the two and, second, a component which comes from the dynamically induced charge on the nearby molecule.

Our objective is to calculate this effective interaction to an accuracy limited only by the accuracy with which we can calculate the energies and excited states of the molecule. The low-lying excited states of the molecule dominate the frequency-dependent part of the effective interaction, while the higher excited states give an appreciable contribution to

the net interaction, but a contribution which is not strongly frequency dependent in our region of interest. This suggests a method of handling the various excited states in the effective interaction which closely parallels a method used within a molecule discussed in II. This method gave good accuracy for low-lying excited states. We wish to retain this accuracy in our calculation of the effective interaction. The method we used there was as follows.

First we carried through a Huckel calculation of the π electron of the molecule and from this obtained a first approximation to the excited energies and molecular orbitals. This allowed a calculation to be made of the effective interaction between electrons within the molecule by summing the bubble diagrams. Using this effective interaction we then obtained the self-consistent-field (SCF) orbitals and energies which were used in a configuration interaction (CI) calculation from which the low-lying singlet excitations were obtained. To do this we divided the single-particle-hole configurations into two sets, *A* and *B*. Set *A* contained the low-lying excitations, and set *B* all the others. The excitations of set *B* were used to calculate an effective interaction for the matrix elements between the configurations of set *A* used in the CI matrix. The justification for this over-all procedure and the results obtained by this means for the absorption spectra of some planar hydrocarbons are described in II.

Our calculation of the effective interaction in this paper follows along similar lines. First we note that the net interaction between two point charges at r_1 and r_2 consists of the sum of the direct Coulomb interaction between the charges located at r_1 and r_2 , and the sum of all possible contributions which result from the virtual excitation of the molecule.

Our calculation of the effective interaction in this paper follows along similar lines. First we note that the net interaction between two point charges at r_1 and r_2 consists of the sum of the direct Coulomb interaction between the charges located at r_1 and r_2 , and the sum of all possible contributions which result from the virtual excitation of the molecule.

Using the above method we obtain the low-lying excitations. However, as pointed out in II [Eq. (10)], these excitations are partially screened by the higher-energy excitations of the molecule, which thus weaken the oscillator strength of the low-lying excitations. The interaction of the external charge with the low-lying excitations can therefore be represented diagrammatically as in Fig. 1(a). At low frequencies which is the region of principal interest to superconductivity, the effective interaction is dominated by these low-lying excitations. For a correct representation of this interaction then it is essential that the frequency depen-

dence arising from these terms be retained. This requires that we know both the excitation energies and their widths. It appears that the widths of the low-lying electronic levels are determined by coupling to the vibrational states of the molecule. Rather than attempt to calculate this, we use the empirically observed widths of these levels in the calculation of the frequency-dependent effective interaction.

In addition to the low-lying excitations, the field of the external charge will be screened by the virtual excitations of the higher-energy configurations. This can be represented as in Fig. 1(b). The frequencies of these excitations in a dye are typically a factor of 3 or 4 greater than that of the principal low-lying level. So that on the time scale appropriate to the low-lying excitations we may treat these higher excitations in the static approximation. This is similar in philosophy to the procedure discussed in II. Our approximation is to use these two classes of diagrams together with the above approximations. By so doing, we retain the accuracy of our earlier results for the low-lying excitations both in regard to their energies and oscillator strengths, and in regard to their frequency dependence. We contribute no error through the use of the empirically observed widths. We take the major contribution of the higher excitations into account in regard to the net interaction, but ignore the weak frequency dependence of this contribution. This yields a tractable procedure which, because of the inclusion of the configuration-interaction calculation, should be appreciably more accurate in determining the frequency-dependent effective interaction in our region of interest than could be obtained by simply sum-

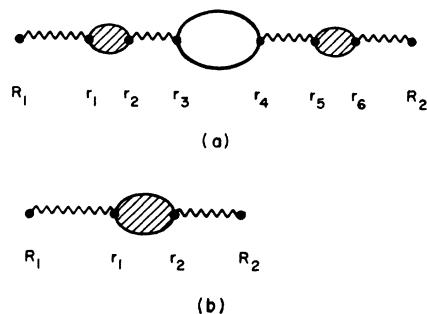


FIG. 1. (a) Diagrammatical representation of the screened interaction (shaded bubble) of an external charge at R_1 with the low-lying excitations of a molecule (open bubble) and the resultant screened response at another external point R_2 . The high-energy excitations alone contribute the screening of the shaded bubble. (b) Diagrammatical representation of the Coulomb interaction between two points R_1 and R_2 lying outside a molecule and the screening (shaded bubble) of this interaction as a result of the high-energy excitations of the molecule.

ming the bubble diagrams for all the configurations. A test of the accuracy of this method cannot be given at this time for it probes details of the interaction which are not accessible to optical measurements. However, inelastic electron scattering experiments⁷ which are currently underway in our laboratory, in principle, can examine these details, and it is hoped that experimental results can be compared with the theory at a later stage.

Using the above approximation together with the rules for describing diagrams, Figs. 1(a) and 1(b) then give the following expression for the frequency-dependent interaction $V(r_1, r_2, \omega)$ in the vicinity of the molecule:

$$\text{Re}V(r_1, r_2, \omega) = V_0(r_1, r_2) + \sum_{r_3, r_4} V_0(r_1, r_3) \Pi(r_3, r_4, \omega) V_0(r_4, r_2), \quad (1)$$

where

$$\Pi(r_3, r_4, \omega) = \sum_A \left(\frac{\omega - E_\nu}{(\omega - E_\nu)^2 + \Gamma_\nu^2} - \frac{\omega + E_\nu}{(\omega + E_\nu)^2 + \Gamma_\nu^2} \right) 2\rho_\nu(r_3)\rho_\nu(r_4) - \sum_B R_{(r_3, r_5)}^{-1} \frac{4' \rho_\mu(r_5)' \rho_\mu(r_4)}{E_\mu}. \quad (2)$$

In (2), Γ_ν is the inverse of the width of the low-lying excitation and the first summation is over the set of configurations lying within the set A. The transition density $\rho_\nu(r_3)$ in the first summation is that given by Eq. (10) of II, i.e.,

$$\rho_\nu(r_1) = \sum_{r_2} R^{-1}(r_1, r_2) \sum_{k, \gamma} {}^{\nu}d_{k\gamma} c_{kr_2} c_{\gamma r_2}. \quad (3)$$

Here ν describes the excited state composed of particle-hole states $|k, \gamma\rangle$ having coefficients ${}^{\nu}d_{k\gamma}$ which are obtained by diagonalizing the CI matrix. Here $R^{-1}(r_1, r_2)$ is the inverse of the matrix \underline{R} defined as in II by the expression

$$R(r_1, r_2) = \delta_{r_1, r_2} + \sum_B \sum_{r'} \frac{4' \rho_\mu(r_1)' \rho_\mu(r')}{E_\mu} V_0(r', r_2). \quad (4)$$

In this summation over the configurations of set B and in that of (2), the transition densities ${}^{\nu}\rho_\mu(r_1)$ are the uncorrected transition densities given by

$${}^{\nu}\rho_\mu(r_1) = c_{lr_1} c_{mr_1}, \quad (5)$$

where the particle-hole configuration $|l, m\rangle$ is labeled μ . The $c_{k,r}$ are the molecular orbital coefficients in the linear-combination-of-atomic-orbitals (LCAO) approximation and k is the state and r the atom.

The contributions to (2) can be understood by noting that the factor \underline{R}^{-1} in (3) contained in ρ_ν in the sum over A, represents the screening due to the

higher configurations of set B in (4) of the coupling to the low-lying excitations. This factor represents the shaded bubbles of Fig. 1(a). The second factor containing the sum over set B represents the direct screening by these higher configurations. The simpler energy dependence of this term results from the static approximation discussed earlier.

The absorption is given by

$$\text{Im}V(r_1, r_2, \omega) = - \sum_{r_3, r_4} V_0(r_1, r_3) \Omega(r_3, r_4, \omega) V_0(r_4, r_2), \quad (6)$$

where

$$\Omega(r_3, r_4, \omega) = \sum_\nu 2\Gamma_\nu \rho_\nu(r_3) \rho_\nu(r_4) \left(\frac{1}{(\omega - E_\nu)^2 + \Gamma_\nu^2} + \frac{1}{(\omega + E_\nu)^2 + \Gamma_\nu^2} \right). \quad (7)$$

In (7) the contribution from higher excited states, i.e., those of set B, give a negligible contribution in the low-frequency region.

These expressions are obtained under the assumption that the interaction of the field with a particular excitation is small compared to $\omega \pm E_\nu$. Where this is violated, other diagrams will contribute to (2) and (6). For a two-level system such as that associated with the principal absorption of a dye, the problem has been solved⁸ for an arbitrary strong interaction. However, the expressions which result are complicated because the stationary states of the dye are themselves seriously perturbed by the interaction. A more useful result can be obtained by noting that under an impulse the dye will in general be left in a configuration which is a linear combination of the ground state ψ_0 and the excited state ψ_1 ,

$$\psi(t) = (1 - a^2)^{1/2} \psi_0 + a e^{-iE_\nu t} \psi_1. \quad (8)$$

As time evolves this results in an oscillation of charge within the dye given by $2a(1 - a^2)^{1/2} \psi_0^* \psi_1 \times \cos E_\nu t$. The amplitude is a maximum when the intensity of the impulse is such as to leave $a = (1 - a^2)^{1/2}$, i.e., $a = 1/\sqrt{2}$. Hence after the impulse, the amplitude of the maximum field at a point R_2 which lies outside the dye, which can be generated by the induced oscillatory charge, is

$$V_{\text{max}}(R_2) = \int \psi_0^*(r_1) V_0(r_1, R_2) \psi_1(r_1) dr_1. \quad (9)$$

When ψ_0 is the ground state and ψ_1 is a singlet excited state, we obtain⁹

$$V_{\text{max}}(R_2) = \sqrt{2} \int {}^{\nu}\rho_{i\alpha}(r_1) V_0(r_1, R_2) dr_1, \quad (10)$$

where ${}^{\nu}\rho_{i\alpha}(r_1)$ has the same meaning as in Eq. (5). We can generalize this result to the case where the higher configurations screen the oscillating field. This causes ${}^{\nu}\rho_{i\alpha}(r_1)$ to be replaced by $\rho_{i\alpha}(r_1)$, as

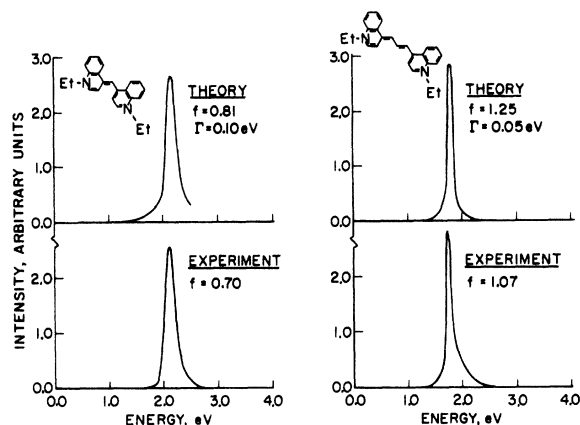


FIG. 2. Theoretical and experimental spectra of the absorption intensity of a 4, 4'-cyanine and a 4, 4'-carbocyanine dye. The ethyl linkage is represented by Et.

given in (3).

The importance of this result is that it gives the maximum screening field that a single level of the dye can produce. Hence it puts a bound on the magnitude of the effective interaction through an expression analogous to (1),

$$V(R_1, R_2) \leq V_0(R_1, R_2) \pm V_{\max}(R_2), \quad (11)$$

where R_1 is the source of the field and R_2 is the field point, and hence an indication when the expressions (2) and (6) break down. Note that the reciprocity between R_1 and R_2 is lost now owing to the saturation of the response of the dye. Later we indicate the magnitude of V_{\max} for the dyes which we have considered.

We have calculated these by direct evaluation of the expression (10). One may note too, that $V_{\max}(R_2)$ can be arrived at approximately from the difference between $V_0(R_1, R_2)$ and $V(R_1, R_2, 0)$ as given by Eqs. (1) and (2). Usually for a dye, the sum over B in (2) is small while the sum over A is dominated by the single strong dye absorption. This

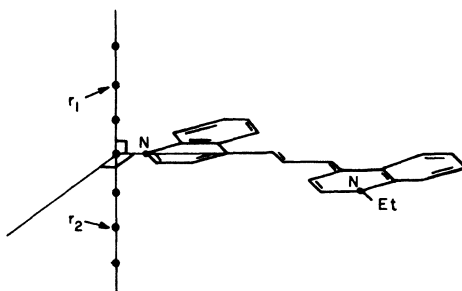


FIG. 3. Orientation of the dye molecule relative to the points r_1 and r_2 used in the computation of the effective interaction.

single term is then approximately $-(2/E_\nu)V_{\max}^2(R_2)$ if R_1 and R_2 are chosen to be equidistant from the dye.

III. NUMERICAL PARAMETERS

In the numerical calculations on the cyanine and carbocyanine dyes we used the following parameters¹⁰: $\alpha_C = -11.2$ eV and $\alpha_N = -24.7$ eV for the Coulomb integrals; $\gamma_{CC} = 10.6$ eV and $\gamma_{NN} = 13.3$ eV for the repulsion integrals; and $\beta_{CC} = -2.3$ eV and $\beta_{CN} = -1.8$ eV for the resonance integrals between atoms within the ring. For the resonance integral between atoms in the conjugated chain, we have used the value of $\beta'_{CC} = -1.4$ eV. This value of β'_{CC} is considerably smaller than the usual value -2.3 eV attributed to the overlap integral between carbon atoms. It was arrived at after trying all other reasonable adjustments of α_N , γ_{NN} , and β_{CN} . None of these adjustments could account for the observed energy of the principal absorption of the dye. However, the use of the single parameter $\beta'_{CC} = -1.4$ eV for the overlap between atoms in the conjugated chain gave the observed energy for each of the cyanines and carbocyanines considered and, as we shall see later, approximately the correct oscillator strengths as well. This strongly suggests that the overlap between the atoms is weaker than for carbocyclic carbons. This result is not surprising, perhaps, in view of the degree of strain and flexibility of this chain.

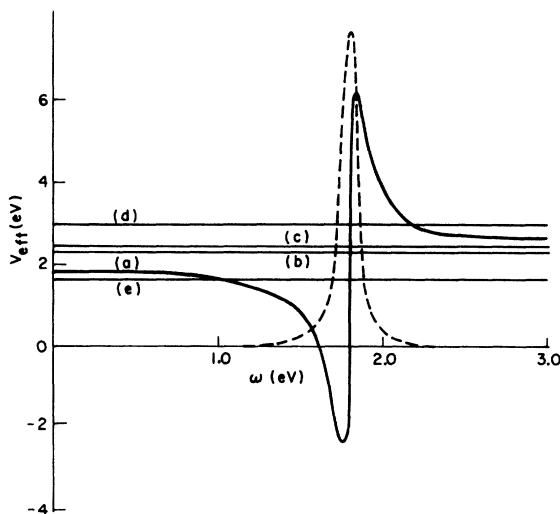


FIG. 4. Effective interaction in the vicinity of the 4, 4'-carbocyanine dye, where r_1 and r_2 are 3 Å above and below the plane of the dye, respectively. Curve (a) is real part of total effective interaction; (b) Coulomb repulsion screened only by higher configuration; (c) unscreened Coulomb repulsion; (d) and (e) limits set by Eq. (11); dashed curve, imaginary part of total effective interaction.

The calculated and observed results for the 1, 1'-diethyl-4, 4'-cyanine and carbocyanine dyes are compared in Fig. 2. The empirical full width at half-maximum of the principal absorption peak was taken from experiment¹¹ and used in the theoretical calculations. The observed oscillator strengths for these transitions given⁹ by $f = 4.315 \times 10^{-9} \int \epsilon d\nu$ were calculated from the data of Mees¹¹ and gave the values shown. The theoretical oscillator strengths derived from the molecular orbital (MO) calculations, on the other hand, gave the theoretical results shown, assuming in each case that the molecules are in their fully extended form. The agreement is reasonable. It should be noted that the screening of the higher $\pi \rightarrow \pi^*$ configurations in general reduces the oscillator strength of the lower transition through the factor $R^{-1}(r_1, r_2)$ in the transition density defined in Eq. (3). This we take into account. The screening of the σ electrons should give a similar reduction. We believe that the remaining difference between the observed and calculated oscillator strengths which amounts to about 15% is due to this σ screening. For while the Piser-Parr-Pople semiempirical parameters¹² take into account σ screening in determining the values of γ_{11} and γ_{12} , they do not take into account the corrections to the oscillator strength which would arise from σ screening through a factor analogous to $R^{-1}(r_1, r_2)$ obtained for the π screening.

IV. RESULTS

We have computed the effective interaction $V(r_1, r_2, \omega)$ between points in the vicinity of several cyaninelike dyes. We thought it would be most useful to consider the situation where r_1 and r_2 lie outside, but near one end of the dye and on a line perpendicular to the plane of the dye, as shown in Fig. 3. The real and imaginary parts of the effective interaction are given by Eqs. (1) and (6), respectively, using the results of the LCAO MO calculation. We have assumed that r_1 and r_2 lie on carbon atoms for which $\gamma_{11} = 10.6$ eV as before.

A typical result is given in Fig. 4 for the carbocyanine dye where r_1 and r_2 are located at a distance of 1.4 Å from the nitrogen atom of the quinoline and 3.0 Å above and below the plane of the dye, respectively.

Curve (a) is the real part of the total effective interaction. Curve (b) represents the Coulomb repulsion screened only by the higher configurations, i.e., those of set B. In each case 16 particle-hole configurations were used in set A and the remaining 100 odd configurations in set B. Curve (c) represents the unscreened Coulomb interaction. The broken curve is the imaginary part of the total effective interaction. The limits set by Eq. (11) are shown at (d) and (e). These will be discussed later.

In Fig. 5 we show the spatial variation of the effective interaction for several frequencies where r_1 is taken in the plane of the dye, 1.4 Å from the quinoline nitrogen, and r_2 is taken at various distances away from r_1 on a line perpendicular to this plane. As the frequency approaches the resonance frequency of the dye (1.79 eV), the effective interaction becomes less and less repulsive and then, just below this frequency, becomes quite strongly attractive over a substantial region near the dye.

It is of special interest to observe how this effective interaction varies as a function of the location of the line $\vec{r}_2 - \vec{r}_1$. In Fig. 6 we show the relative strength of the contribution from the low-lying excitations to the effective interaction for r_1 and r_2 lying on a line perpendicular to the plane of the dye and passing through each of the points shown. In each case this line is located a typical bond length 1.4 Å from the nearest atom in the dye. It is interesting to note that the contribution to the effective interaction is not strongly peaked near the nitrogen atom, but is relatively constant near the entire end of the dye. Chemically, this is important since the attachment to the conductive spine need not be made at the nitrogen site, but rather could be made at the more accessible carbon site on the adjacent ring.

Finally, we show in Fig. 7 the real part of the effective interaction for the three dyes, the cyanine, carbocyanine, and dicarbocyanine dyes. In Fig. 8, $n = 0, 1, 2$.

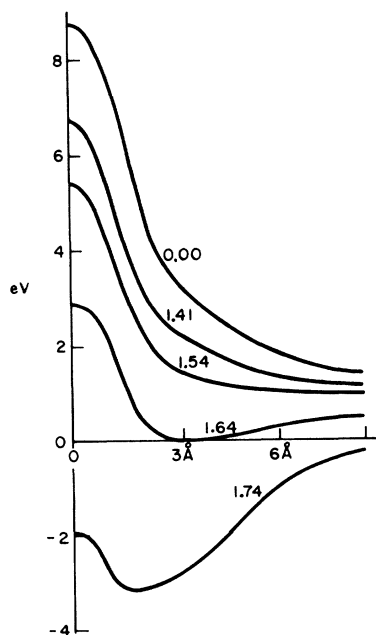


FIG. 5. Spatial variation of the effective interaction near the carbocyanine dye along the line $r_1 r_2$ at various frequencies, 0.00, ..., 1.74 eV.

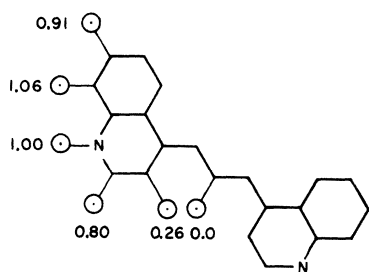


FIG. 6. Relative strength of the contribution from the low-lying excitations to the effective interaction for $r_1 r_2$ passing through the given points near the carbocyanine.

This shows rather clearly that the effective interaction becomes more strongly attractive as the transition dipole of the molecule is made larger with increasing length of the conjugated chain.

V. DISCUSSION

From the comparison of the experimental and theoretical results of the oscillator strengths and energies, it appears that one can calculate these to an accuracy of about 15%. This was done by adjusting the overlap integral β'_{CC} for the atoms in the conjugated chain of the dye to obtain the correct energy for one such dye. Approximately the correct energy for the principal absorption and the correct oscillator strength were then obtained for several related dyes. In each case, the theoretical calculations overestimate the oscillator strengths by about 15%. We attribute this to the neglect of σ screening

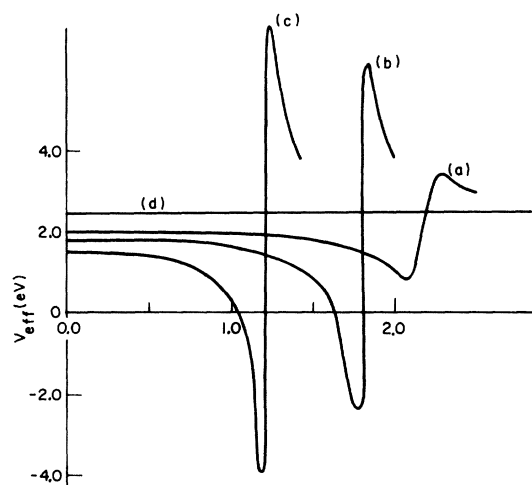


FIG. 7. Comparison of the real part of the effective interaction near (a) the cyanine, (b) the carbocyanine, and (c) the dicarbocyanine. Here (d) is the unscreened Coulomb interaction. Points r_1 and r_2 are 3 Å above and below the plane of the dye and 1.4 Å from the quinoline nitrogen.

of the transition dipole. By correcting the theoretical oscillator strength by a factor of 0.85 to take this into account, close agreement can be obtained for the oscillator strengths in each case. The approximate agreement of these oscillator strengths, however, does not give us any direct information on the transition densities themselves, but only on their dipole average. However, it is reasonable to believe that the molecular orbital treatment which gives agreement to this accuracy should also give approximately the correct transition densities as well. On the basis of this belief, we can attribute an accuracy of about 15% also to the values obtained for the effective interaction, for this depends upon the transition density to the same order as does the oscillator strength. As indicated earlier, a direct measurement of these transition densities would be valuable as a check against the theory, and experiments⁷ on these lines are currently under way.

At this accuracy, the results are close enough to the observed quantities for the theory to be useful as a guide to both the choice of dye and the choice of a point of attachment.

For the three dyes considered, $n = 0, 1, 2$ of Fig. 8, the maximum screening field given by Eq. (10), with ρ replacing ρ' at the points considered in Figs. 4 and 7, was found to be 0.56, 0.65, and 0.67 eV, respectively. For a single dye, this represents an upper limit on the attractive component at these points. However, in a repeated structure formed by an array of dyes where the two electrons, which interact via this effective interaction, have their wave functions distributed over many unit cells, this limitation no longer applies. In that case, each dye is weakly polarized by the distributed electron charge, and the screening field is the sum of the contributions from each dye. The upper limit on this screening field is then the sum of the maximum contributions from each dye. Roughly speaking then, it would appear from Fig. 7 that three or four dyes would be needed over the 6-Å region between r_1 and r_2 to obtain a net attractive component large enough to cancel the Coulomb repulsion of 2.26 eV. The dyes, of course, will interact with one another, and hence the exact behavior would be rather com-

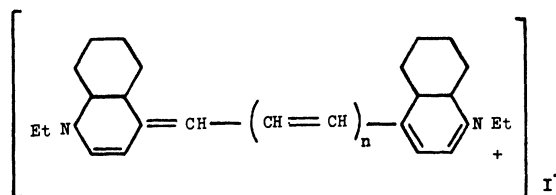


FIG. 8. The three dyes considered: the di-ethylcyanine, -carbocyanine, and -dicarbocyanine iodide dyes ($n = 0, 1, 2$). The ethyl linkage is represented by Et.

plicated. At this point it appears that something of the order of three or four dyes would be needed for each pair of electrons, in order to obtain an attractive interaction in the conductive pathway.

In regard to the question of superconductivity, it should be noted that it is the contribution of the Coulomb pseudopotential which plays the role ultimately in determining the effective interaction at low frequencies in the energy-gap equation, rather than the Coulomb potential itself. It may be recalled that in the BCS energy-gap equation¹³ the repulsive interaction at high frequencies introduces correlations between the pairs such that the effective Coulomb pseudopotential U_C is reduced below the Coulomb interaction V_C [curve (b) of Fig. 4] by a factor of the order of $1/[1 + V_C N(0) \ln(E_B/E_D)]$, where E_B is

approximately the width of the conduction band, $N(0)$ the density of states at the Fermi surface, and E_D , in this case, the energy of the dye absorption, rather than the Debye energy. This factor could reduce somewhat the restrictive conditions discussed above; however, by the same argument, any repulsive contribution which might arise at very low frequencies from vibrational or phonon modes would have the opposite effect and, depending on the band structure of the conduction electrons, might well dominate. So it is impossible at this stage to determine whether or not the effective interaction could be attractive without taking into account these details and the effects of interactions between the dyes. We leave these considerations to a later paper.

*Work supported in part by the Advanced Research Projects Agency, Washington, D. C. and the U. S. Office of Naval Research.

¹H. Gutfreund and W. A. Little, Phys. Rev. **183**, 68 (1969).

²H. Gutfreund and W. A. Little, J. Chem. Phys. **50**, 4468 (1969).

³H. Gutfreund and W. A. Little, J. Chem. Phys. **50**, 4478 (1969).

⁴W. A. Little, Phys. Rev. **134**, A1416 (1964).

⁵W. A. Little, J. Polymer Sci. C **29**, 17 (1970).

⁶K. F. G. Paulus, Mol. Phys. **10**, 381 (1966).

⁷S. Gerber, J. Polymer Sci. C **29**, 211 (1970).

⁸N. F. Ramsey, *Molecular Beams* (Oxford U. P., Oxford, England, 1956), p. 118.

⁹L. Salem, *The Molecular Orbital Theory of Conjugated Systems* (Benjamin, New York, 1966), pp. 358-359.

¹⁰For a definition of these terms see Ref. 1.

¹¹K. Mees, *The Theory of the Photographic Process* (MacMillan, New York, 1942), p. 1002.

¹²R. Pariser, J. Chem. Phys. **21**, 568 (1953).

¹³J. R. Schrieffer, *Theory of Superconductivity* (Benjamin, New York, 1964), p. 187.